7th CNS International Steam Generators to Controls Conference
Toronto, Ontario, Canada, November 11-14, 2012

Investigation of the Integrity of U-Bend Tube Bundles Subjected to Flow-Induced Vibrations

Marwan Hassan[1] and Jovica Riznic[2]

[1]University of Guelph, Ontario, Canada

[2] Canadian Nuclear Safety Commission, Ontario, Canada

ABSTRACT

Maintaining the integrity of nuclear steam generator (SG) tubes in CANDU reactors is a major safety issue since they maintain the physical barrier between the primary and secondary coolants. The integrity of these tubes can be compromised due to flow-induced vibrations in the form of fatigue and fretting wear damage. Wear is a result of the tube impacting and sliding against its loose supports, and it becomes more severe as the tube/support clearance increases. The vibration is caused by fluid flow around these tubes through turbulence and fluidelastic instability mechanisms. Supports are installed to stiffen the structure and to ensure safe and stable operation. The U-bend region is the most critical part since it is subjected to high cross flow. Therefore, special attention is paid to properly supporting this region. However, in some situations, tube support plates (TSP) located on the straight part of the tube may deteriorate to the point where extremely large clearances, or even total wastage of the supports, may result. One possible cause for such a situation is corrosion and/or excessive fretting wear. This loss of TSP may affect the rate of wear in the U-bend portion of the tube due to the increased flexibility in this region. The integrity could be seriously breached as result of a potential support loss. This paper addresses the flow-induced vibrations (FIV) aspect, consequences, and suggested remedies for support degradation. This analysis will include fretting wear producing parameters, such as impact force and normal work rate. Turbulence and fluidelastic instability (FEI) are considered to be the main excitation mechanisms. The investigation is conducted through a numerical simulation of the full U-bend tube bundles including modelling the variable flow distribution, flow excitation, impact, and friction at the supports.

1. INTRODUCTION

Steam generators have experienced problems related to tube failure. While many of these failures have been attributed to corrosion, it has been recognized that flow-induced vibrations have also contributed significantly to tube failure. Tube vibrations are generated by external cross-flow. These vibrations cause damage over a relatively short time if vortex shedding resonance or fluidelastic instability occur. The latter may be especially destructive. In order to avoid these excessive vibrations, tubes are stiffened by placing supports along their length. Various tube/support geometries have been used (see for example, Weaver & Schneider 1983 [1]), but the majority are either support plates (plates with drilled or broached holes) or flat bars. Due to manufacturing considerations, clearance between the tubes and their supports is often considered necessary. As a result, the effectiveness of the tube support could be compromised. A combination of flow-induced turbulence and fluidelastic forces may then lead to excessive tube vibration at the supports.

While large-amplitude fluidelastic instability can be avoided by choosing the proper location and number of supports, the tubes may still vibrate inside their support space due to turbulence and per-stability fluidelastic excitation. These vibrations cause the tube to impact against and/or slide along the support, which leads to gradual fretting wear damage. Under normal circumstances in well-designed nuclear steam generators, tube wear will not exceed the safety limits (40% of the wall thickness) during the life of the steam generator. Still, there is an increase in the clearance between the tubes and their supports, which in turn, could decrease the effectiveness of the support through unacceptable fretting wear and loss of stability. Clearances for manufacturing considerations should therefore be kept as small as possible. Gradual fretting wear and chemical cleaning can also contribute to an increase in the clearances. This situation, however, should be accounted for at the design stage.

Another source of clearance enlargement is the degradation of the tube support plate. This degradation may be caused by flow-accelerated corrosion of the support plate. In severe circumstances, a complete loss of the TSP ligaments may occur. This loss of TSP ligaments results in a lack of support for the adjacent tubes, making them more susceptible to fretting-wear damage and fatigue cracking at these locations. In addition, this may affect the rate of wear in the U-bend portion of the tube due to the evolution of unstable modes.

This paper addresses the consequences of support loss in a tube support in the straight portion of a typical CANDU U-bend steam generator tube. In addition, an evaluation of the suggested remedies is presented. The evaluation is presented in terms of the normal work rate, which is the main wear producing parameter.

2. MODELLING

2.1 Tube Structural Model

Figure 1a shows the structural configuration of the U-bend tube. In each of the straight portions, the tube is supported by seven broached-hole supports. The tube is supported by scalloped-bar supports in the U-bend. The straight portions of the tube are mainly exposed to axial flow while the U-bend portion is exposed to a non-uniform cross-flow. The tube's outer and inner diameters are 13.02 mm and 10.76 mm, respectively. The full tube model (Figure 1b) is developed using elastic straight beam elements. The U-tube consists of 112 elements in the straight region and 79 elements in the U-bend region, as shown in Figure 1b. The velocity distribution shown is a result of flow stability and fouling calculations that were performed at AECL using the THIRST (Thermal-Hydraulics In Recirculating STeam generator) code (Heppner et al., 2006). The flow velocity and the density distributions are adopted from the available data in the literature [2]. The boundary conditions at the tube sheet nodes are fixed, but the nodes at the tube support plates and the anti-vibration bars are free to move in the axial direction.

2.2 Fluid Loading

Turbulence and fluidelastic excitations are considered in this analysis. Random turbulence excitation is a significant vibration mechanism in tubes subjected to cross-flow. The interior tubes within a tube bundle are excited by the turbulence generated within the bundle. In general, fluid excitation due to turbulence is modelled as randomly distributed forces. To implement this approach, the empirically based bounding spectra of turbulence excitation are obtained using the flow velocity, the tube diameter, and the array geometry. The bounding spectra proposed by Oengören and Ziada [3] are used to simulate the random excitation forces.

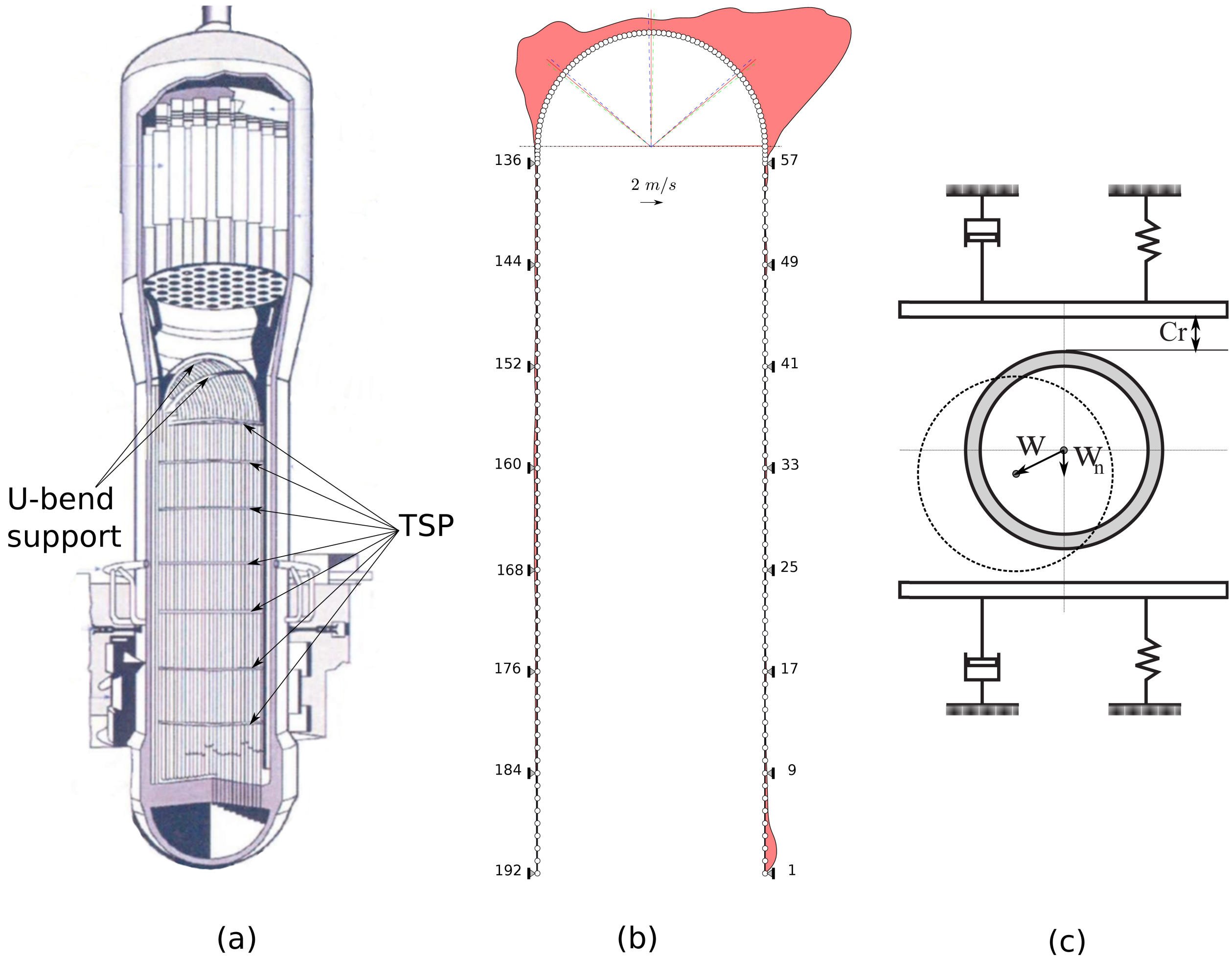

Figure 1: Nuclear steam generator: (a) a typical overall view, (b) finite element model and flow distribution, (c) tube/support impact mode.

The fluidelastic instability model utilized in this work is the flow-cell model described in detail by Hassan et al. in a series of papers [4-7]. Briefly, the entire flow inside the tube bundle is divided into a number of layers, each of which is associated with a tube finite element. The flow inside each layer can be idealized by a series of flow channels. The area of these flow channels is decomposed into a steady state component and a perturbation component. The area perturbation is set to the tube lift displacement along the tube-flow channel contact length. The response history is required in order to calculate the area perturbation in the channel. Now, the displacement at each element is needed to calculate the area perturbation. The area perturbation at any given location (s) is equal to the displacement at t-$\tau(s)$. The time lag $\tau(s)$ is calculated using the flow velocity U_o, and the location s as $\tau(s)=\gamma s/U_o$. Using the unsteady continuity and momentum equations, the flow velocity and pressure can be obtained at any point in the flow channel. The fluidelastic forces per unit length are evaluated by integrating the pressure along the tube/channel interface. The fluid forces are then treated as a distributed pressure, and the consistent load vector F_f is obtained. Now the newly estimated fluidelastic force vector, along with the impact force vector, are added to the global load vector and checked for convergence. The tube response at the support node is used to calculate the impact force. Upon convergence, the updated displacement, fluidelastic forces, and contact forces are stored. This process is repeated at each time step. Calculating the fluidelastic instability forces using this method does not require knowing the instantaneous vibration frequency.

2.3 Tube-Support Impact Modelling

The mathematical modelling of the tube/support impact used herein was described in detail and verified by Hassan et al. [8]. Briefly, the tube is discretized into finite beam elements, and the proper boundary conditions are applied. Any loose support configuration can be modelled by a number of massless bars arranged around the tube. Each bar is supported by an equivalent contact spring and damper (Fig. 1c). If the normal component of the tube displacement (w_n) exceeds the radial support clearance (C_r), contact takes place. The normal contact forces are calculated in each bar by evaluating the elastic ($K_c(w_n-C_r)$) and damping ($1.5\beta K_c\ (w_n-C_r)\ dw_{n/}dt$) forces in the spring and the damper. K_c and β are the spring stiffness and the material-damping coefficient respectively. The force balance friction model was used to compute the shear contact forces.

3. ANALYSIS

3.1 Vibration Modes

Mode shapes for the first in-plane and out-of-plane modes are shown in Figure 2. The Configuration 1 modes shown here are estimated by assuming that all the supports are effective. The effect of the added mass due to both the internal and external flows is included in the natural frequencies and the mode shapes. These mode shapes agree well with those reported by Mohany et al. [9] for a similar geometry. The loss of support H07 (Configuration 2) resulted in a significant decrease in the in-plane natural frequency (from 37 Hz to 28 Hz) and a slight decrease in the out-of-plane natural frequency (from 56 Hz to 55.5 Hz). The addition of the flat bars F1 and F2 (Configuration 3) resulted in a major increase in the out of plane natural frequency (from 55.5 Hz to 97.5 Hz).

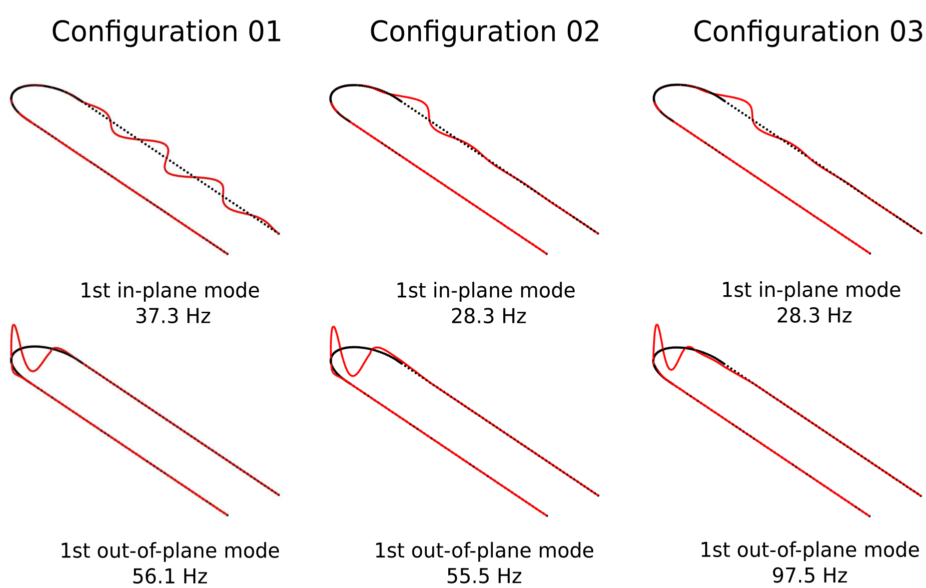

Figure 2: Linear mode shapes.

3.2 Linear Simulations

The main objective of the linear simulations is to investigate the linear stability threshold. Catastrophic failure may occur if the stability threshold is exceeded. Therefore, an accurate prediction of the critical flow velocity is important. This is accomplished by numerical simulations in which the flow velocity is varied and the resulting response is observed. A number of simulations were conducted where the inlet flow velocity ratio U_r is varied in the range of 0.1 to 2.0, and the rms lift displacement is calculated for each of these velocities. The velocity ratio is the ratio of the flow velocity to the rated flow velocity at full load. Figure 3a depicts the rms out-of-plane response at the first span of the U-bend as a function of the velocity ratio. For all velocity ratios, a very low turbulence force level was used to enhance the illustration of the FEI effect. The response shows a characteristic behaviour where for a range of velocity ratios (1-1.5), the response gradually increases due mainly to turbulence excitation. The onset of instability is found to be at a velocity ratio of 1.5, where a larger rate of response increase occurs. The fluidelastic instability margin is therefore 1.5, which is similar to the engineering factor of safety.

Stability charts are always expressed in terms of the dimensionless flow velocity ($U_{cr}=U_c/fd$) and the dimensionless mass damping parameter (*MDP*). The mass-damping parameter (*MDP*) is defined as:

$$MDP = \frac{\delta \int_0^L m(\phi(x))^2 dx}{d^2 \int_0^L \varrho(x)(\psi(x))^2 (\phi(x))^2 dx}$$

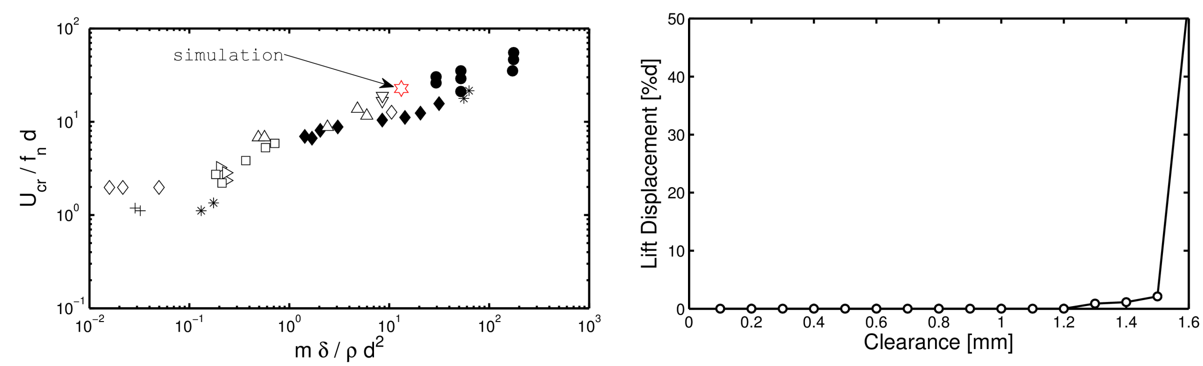

Figure 3: Linear simulations; (a) predicted tube rms response vs. flow velocity, (b) the predicted critical flow velocity vs. available experimental data.

where m and δ are the tube mass per unit length and the structural damping logarithmic decrement, respectively. The velocity distribution may be written as $V\varphi_i(x)$. $\phi_i(x)$ is the amplitude distribution or mode shape function. The effective velocity, V_i, is computed for each mode and the minimum value is the critical velocity. For Configuration 1, the mass damping parameter for the critical mode is 13.2 (first out-of-plane mode).

Figure 3b shows the predicted critical flow velocities and the experimental stability data reported from the literature. The comparison in this figure reflects the fact that the predicted critical flow velocities are in reasonable agreement with the experimental results.

3.3 Nonlinear Simulations

The linear response of a tube is generally dominated by the fundamental mode. Due to the clearance at the supports, tube dynamics are not well defined in terms of the natural frequencies and mode shapes.

Three configurations were simulated (Figure 4). In the straight portions, the tube is supported by broached hole supports (H01, H02, ... H07, and C01, C02, ... C07), in which the letters C and H refer to the cold leg side and the hot leg side, respectively. In addition, there are three sets of scallop bar supports (S1, S2, S3). Each scallop-bar support set consists of two bars (A and B) each of which contains a half-circle drilled hole support space. Such a configuration (Config01) is shown in Figure 4a, which is the original configuration.

Configuration 2 is shown in Figure 4b. This configuration is identical to Configuration 1 except that it does not have the broached-hole support H07. This is meant to represent the full loss of support H07. Configuration 3 is shown in Figure 4c, which represents the addition of two flat bar supports (F1 and F2) to remedy the loss of H07. Additional flat bars at the H07 location (support comb) were also used to remedy the loss of support H07.

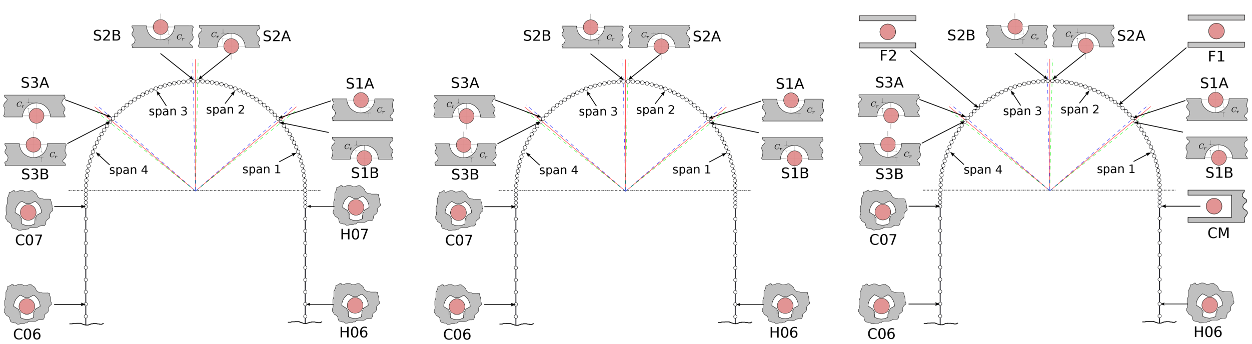

Figure 4: Nonlinear model configurations: (a) Configuration 1, (b) Configuration 2, (c) Configuration 3.

3.3.1 Configuration 1

A simulation series of Configuration 1 (Figure 4a) were conducted while keeping all support clearances at 0.1 mm. However, the clearance at H07 was varied from 0.1 mm to 1.5 mm. Figure 5a shows the predicted work rate as a function of the radial clearance. The general behaviour of the work rate generated at the scallop bar supports is the same for all clearances under consideration. A gradual increase in the work rate was observed with an increase in the hot and cold leg broached hole support clearances. In contrast to the scallop bars, an increase in the broached-hole support clearance resulted in a decrease in the work rate at these supports. Although the clearances at all of the 14 broached holes are considered, only the results for H07 and C07 are presented. The work rate is found to vary from 12.5% to 16.6% among the scallop bars. In addition, the work rate at the scallop bars increases by 228% when the clearances at the broached support are increased from 0.1 mm to 0.9 mm.

Figure 5b shows the work rate results for supports H07 and S2A. All support clearances remain at 0.2 mm, except for that of H07, which was varied. A similar trend was observed where an increase in the H07 clearance resulted in a work rate increase at support S2A and a work rate decrease at support H07. However, the resulted work rates are twice as high as those of the 0.1mm case.

When the radial clearance of all supports is uniform, the differences in the work rate are small. When the clearance at one support is enlarged and the clearances of the remaining supports are constant, the normal work rate in these supports increases. The fretting wear is proportional to the work rate; hence, an increase in the work rate increases the fretting wear rate. As stated earlier, a normal work rate in the order of a few mW may be considered a good indication of a well-designed heat exchanger. However, a reasonable work rate value is dependent on the wear coefficient. Unacceptable levels of normal work rates are attributed to large clearances at all the supports. If the support clearance in the U-Bend region is kept under 0.2 mm, the normal work rates would be within the < 20 mW range even if there has been a total loss of support H07. To maintain a normal work rate of a few mW at all supports, the clearance at these supports must be kept below 0.1 mm.

Configuration 2 represents the total degradation of support H07. While this analysis is conducted to address a generic CANDU steam generator case, some operating steam generators have experienced degradation at supports HO6, and HO5 as well, with H07 being the worst. Degradation was also observed at the lowest plates, but it was not as extensive as that at the intermediate and high plates. Results for Configuration 2 are equivalent to those of Configuration 1 when considering clearances larger than 1.3mm for H07. The work rate results for Configuration 2 are approximately twice those of the original configuration. This leads to an accelerated rate of fretting wear.

3.3.2 Configuration 3

To simulate this situation, support H07 was removed to reflect the full degradation of this support. The flat bars, F1 and F2, and the support comb, CM, (at the H07 location) are added to reflect the remedies followed (Figure 4c). A series of simulations were conducted using the following assumptions:

• The radial clearance of the hot side was set to increase linearly with the support location. The clearance at H01 is set to the nominal radial clearance of 0.2 mm, and to a maximum value of 3.5 mm at H06. This was done to simulate the progression of support degradation on the hot side.

• The radial clearance at the comb support is set to 0.27 mm (conservative value).

• The radial clearance at the broached hole supports along the cold leg are set in accordance to the original design's average value of 0.2mm.

3.3.2.1 Case 1

These simulations were carried out using the above assumptions, with variations in the clearance of the scallop bars S1A-S1B, located at 40^{o} in the U-bend, ranging from 0.1 mm to a very high value of 1.5 mm. The design radial clearance of 0.2 mm is considered for all supports. The resulting normal work rate at supports S1A-S1B decreases as the radial clearance increases. These supports lose contact at radial clearances ≥ 0.5 mm. The other supports experience an increase in the normal work rate as the support clearance increases, then the normal work rate becomes constant at radial clearances ≥ 0.5 mm. The highest work rate was found at the scallop bars (S2A-S2B) located at the U-bend apex. Figure 6a shows a representative example of this trend (results for the flat-bar support).

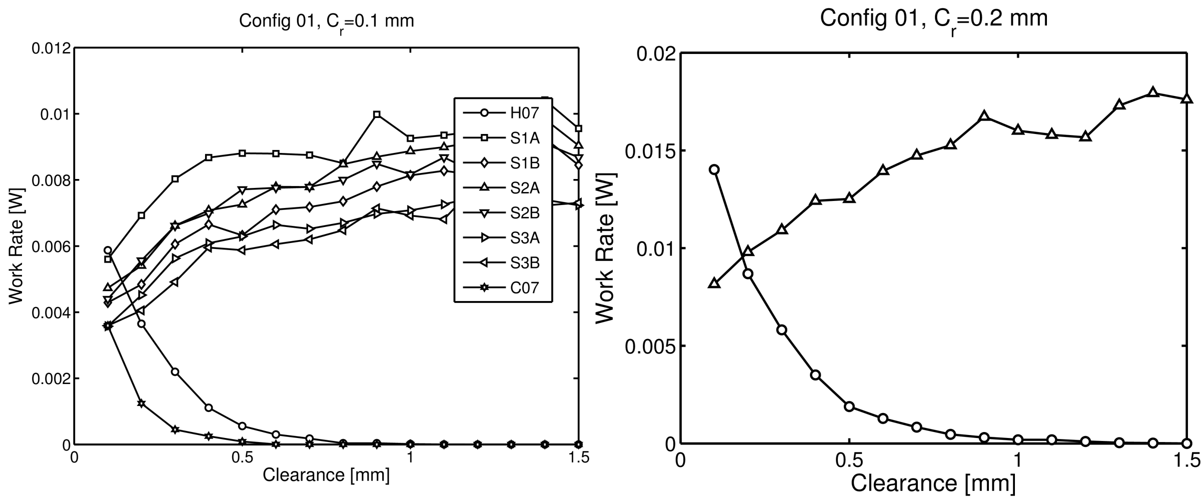

Figure 5: Work rate results for Configuration 1 varying H07 clearance : (a) U-bend clearance = 0.1 mm, (b) U-bend clearance = 0.2 mm.

3.3.2.2 Case 2

A second set of simulations was conducted using the same assumptions and varying the clearance at Flat Bars F1 and F2. Normal work rates at the flat bars decrease as the support clearance increases, with a total loss of contact at radial clearances ≥ 0.5 mm. Similar to the previous case, an increase in the radial clearance at the flat bars results in an increase in the work rate at all the supports. This occurs up to a radial clearance of 0.4 mm beyond which the work rate levels off. An example of this behaviour is manifested in Figure 6b, which depicts the work rate results at the scalloped-bar support S1A.

3.3.2.3 Case 3

A third set of simulations was conducted using the same assumptions and varying the clearance at scallop bars S2A and S2B, which are located in the apex of the U-bend. Normal work rates at scallop bars S2A and S2B decrease as the support clearance increases. A total loss of contact with any of the supports in the U-bend was, however, not observed. The increase in the work rate at all the supports is much more dramatic. An example of this behaviour is shown in Figure 6c. An increase in the radial clearance from a nominal value of 0.2 mm to a large value of 1.5 mm results in an increase in the normal work rate in the flat bar (F1) from 5.15 mW to a value of 68.81 mW. This 13-fold increase in the work rate is deemed devastating.

To summarize the results of the previous three cases, if the clearances are kept within the appropriate design values (all U-Bend supports, including the comb support at H07, are at a value of 0.2 mm or less), the normal work rate values are in the order of a few mW, which is considered to be a reasonable value. The degradation of Scallop Bars 1 or 3 did not result in a dramatic change in the normal work rate. This is attributed to the fact that the additional flat bars F1 and F2 are in the vicinity of the scallop bars, which helped in stabilizing and supporting the system at these locations. Similar results were obtained when the clearance was enlarged at the flat bars. It was shown that the degradation of the scallop bars at the apex of the U-Bend proves to be critical for the system. The clearance of the scallop bars at the apex must be kept below 0.3 mm in order for the work rate to remain within a few mW.

The rms bending stress distribution along the tube length was also studied. It was found that the U-bend region represents higher bending stress values. The support clearance, however, has a significant effect on the stress level and a smaller effect on the trend. The maximum stress value of 6.0 MPa was recorded at Scallop Bar 2. These values are very small compared to the fatigue strength of the tube material, and therefore fatigue failure is not expected.

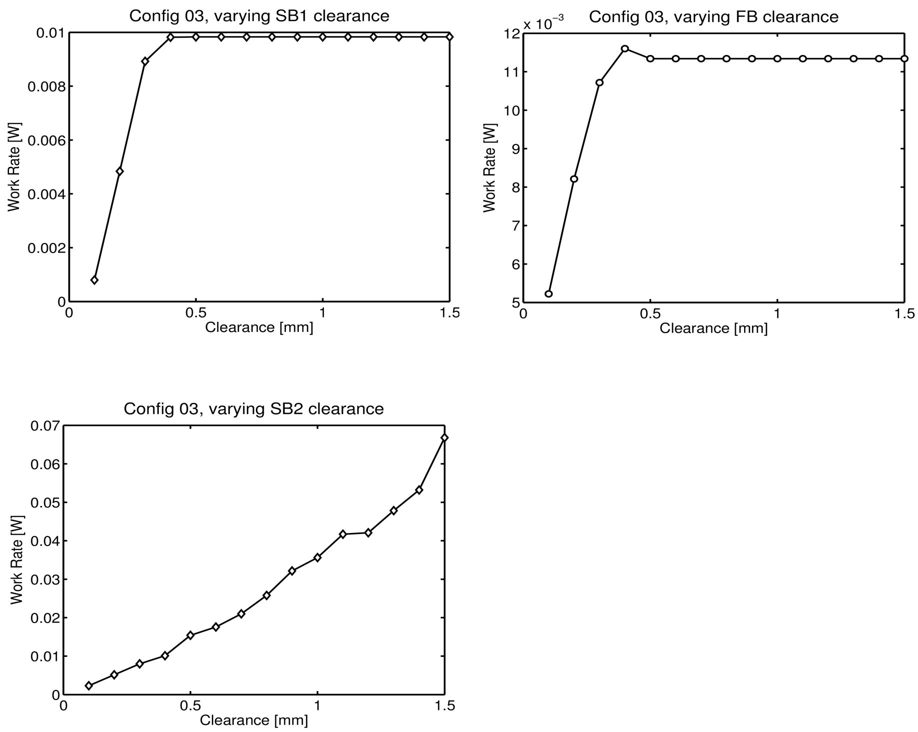

Figure 6: Work rate results for configuration 3 : (a) case 1, effect of varying the clearance at the scallop bars S1, (b)case 2, effect of varying the clearance at the flat bars F1(c) case 3, effect of varying the clearance at the scallop bars S2.

4. SUMMARY

Simulations of flow-induced vibrations in a full scale U-bend tube bundle typical of a CANDU steam generator design were presented. The simulations considered the combined effect of turbulence and fluidelastic instability excitation. The model includes a U-bend tube supported by 14 broached-hole, 6 scallop-bar, and 2 flat-bar supports. The flow is non-uniform in both the velocity and the density distribution. The flow distribution was obtained from thermal-hydraulic analysis previously carried out by AECL. Simulations were conducted to investigate the effects of support radial clearance and support offset. The following conclusions are made:

- The loss of support H07 results in an increase in the work rate at the U-bend supports. The scale of the increase is dependent on the average radial clearance. If the support clearance in the U-Bend region is kept well under 0.1 mm, the normal work rates will be within relatively moderate levels.

- The addition of the flat bar stabilizes the tube bundle. If the clearances of all U-Bend supports, including the comb support at H07, are kept within the design value of 0.2 mm, the normal work rate values are in the order of a few mW, which is considered a reasonable value. The degradation of Scallop Bars 1 or 3 did not result in a dramatic change in the normal work. This is attributed to the fact that the additional flat bars F1 and F2 are in the vicinity of the scallop bars, which helped in stabilizing and supporting the system at these locations. Similar results were obtained when the clearance was enlarged at the flat bars.
- It was shown that the degradation of the scallop bars at the apex of the U-Bend proves to be critical for the system. The clearance of the scallop bars at the apex must be kept below 0.3 mm in order for the work rate to be within a few mW.

5. REFERENCES

1. Weaver, D. S. and Schneider, W. The effect of flat bar supports on the crossflow induced response of heat exchanger U-tubes. ASME Journal of Pressure Vessel Technology 105, 775–781, 1983.
2. Heppner, K., Laroche, S. and Pietralik, J. The THIRST Chemistry Module as a Tool to Determine Optimal Steam Generator Corrosion Control Strategies, CNS International Steam Generator Conference, Toronto, Canada, November 26-29, 2006.
3. Oengören, A. and Ziada, S. Flow periodicity and acoustic resonance in parallel triangle tube bundles. Journal of Fluids and Structures, 14(2):197–219, 2000.
4. Hassan and M. Hayder. Modelling of fluidelastic vibrations of heat exchanger tubes with loose supports. Nuclear Engineering and Design, 238(10):2507 – 2520, 2008.
5. Hassan, M. and Achraf, H. Time domain models for damping-controlled fluidelastic instability forces in tubes with loose supports. ASME Journal of Pressure Vessel Technology, 132(4):041302, 2010.
6. Hassan, M., Gerber, A. and H. Omar. Numerical estimation of fluidelastic instability in tube arrays. ASME Journal of Pressure Vessel Technology, 132(4):041307, 2010.
7. Hassan, M. and Mohany, A. Characterization of Flow-Induced Vibration and Fretting Wear Potential in Nuclear Steam Generator Tube Bundles, ASME Pressure Vessels and Piping Conference, Paper no. PVP2011-57182 pp. 141-149, July 17–21, 2011, Baltimore, Maryland, USA, 2011.
8. Hassan, M., Weaver, D., and Dokainish, M. A simulation of the turbulence response of heat exchanger tubes in lattice-bar supports. Journal of Fluids and Structures, 16(8):1145–1176, 2002.
9. Mohany, A., Janzen, V., Feenstra, P., and King, S. "Experimental and Numerical Characterization of Flow-Induced Vibration of Multi-Span U-Tubes", ASME J. Pressure Vessel Technol., 134, 011301, 2012.